First measurement of proton decay from a transfer reaction to ²¹Na

M. J. Kim (김민주), K. Y. Chae (채경육), S. Ahn (안성훈), D. W. Bardayan, S. M. Cha (차수미), K. A. Chipps, 2.4.5
J. A. Cizewski, M. E. Howard, R. L. Kozub, K. Kwak (곽규진), B. B. Manning, M. M. Matos, P. D. O'Malley, 6.3
S. D. Pain, W. A. Peters, S. T. Pittman, A. Ratkiewicz, M. S. Smith, S. and S. Strauss, and S. Strauss, sungkyunkwan University, Suwon 16419, Republic of Korea

Department of Physics and Astronomy, University of Tennessee, Knoxville, Tennessee 37996, USA

Department of Physics, University of Notre Dame, Notre Dame, Indiana 46556, USA

Colorado School of Mines, Golden, Colorado 80401, USA

Physics Division, Oak Ridge National Laboratory, Oak Ridge, Tennessee 37831, USA

Department of Physics and Astronomy, Rutgers University, New Brunswick, New Jersey 08903, USA

Department of Physics, Tennessee Technological University, Cookeville, Tennessee 38505, USA

Department of Physics, School of Natural Science, Ulsan National Institute of Science and Technology (UNIST),

Ulsan 44919, Republic of Korea

⁹Department of Physics and Astronomy, Louisiana State University, Baton Rouge, Louisiana 70803, USA

¹⁰Oak Ridge Associated Universities, Oak Ridge, Tennessee 37831, USA

(Received 4 April 2021; revised 21 June 2021; accepted 20 July 2021; published 29 July 2021)

Decay protons from excited states in 21 Na populated through a previously reported 24 Mg(p, α) 21 Na transfer reaction [Cha *et al.*, Phys. Rev. C **96**, 025810 (2017)] were analyzed to extract the proton branching ratios of the energy levels. By utilizing 31-MeV proton beams from the Holifield Radioactive Ion Beam Facility of Oak Ridge National Laboratory and isotopically enriched 24 Mg solid targets, the decay protons were detected in coincidence with α particles from the (p, α) reaction using a silicon strip detector array. Proton decay branching ratios of several 21 Na levels were deduced for the p0 and p1 decay channels to the ground and first excited states in 20 Ne, respectively.

DOI: 10.1103/PhysRevC.104.014323

I. INTRODUCTION

Transfer reactions provide a powerful tool in nuclear spectroscopy studies. By measuring the energies and angular distributions of reaction products, critical properties of the populated levels such as the excitation energies, spins and parities, and spectroscopic factors can be extracted. As well summarized in Ref. [1], various types of single- and multinucleon transfer reactions, including (p, d), (p, t), $({}^{3}\text{He}, d)$, and $({}^{3}\text{He}, n)$, were utilized to study the structure of the nuclei in normal and inverse kinematics. When energy levels above particle thresholds are populated through transfer reaction experiments, measuring the properties of particle decay channels may also provide useful information such as branching ratio and angular correlations for states, as previously shown in Refs. [2–7].

The $^{24}{\rm Mg}(p,\alpha)^{21}{\rm Na}$ transfer reaction in normal kinematics was previously performed to study the spectroscopy of the radionuclide $^{21}{\rm Na}$ [8]. A total of 12 $^{21}{\rm Na}$ energy levels were identified at energies less than $E_x=7.2$ MeV, of which 2 levels located at 6.594 and 7.132 MeV were observed for the first time. The empirical angular distributions of reaction α particles were compared with distorted-wave Born approximation (DWBA) calculations to

constrain the spin and parity assignments of populated levels. Using the spectroscopic information, the astrophysical $^{17}F(\alpha,p)^{20}Ne$ reaction rate was obtained at temperatures relevant to x-ray bursts. In the present work, the measurement of proton decay from ^{21}Na levels, which were populated from the transfer reaction, is reported as a follow-up analysis.

The branching ratios of energy levels often play important roles in nuclear reaction rate calculations. In recent work by Lalanne et al. [9], for instance, the ${}^{37}\text{Ca}(p, d)\,{}^{36}\text{Ca}$ reaction was measured at the Grand Accelerateur National D'Ions Lourds facility using a radioactive beam of ³⁷Ca and a liquid hydrogen target to study the $^{35}{\rm K}(p,\gamma)$ $^{36}{\rm Ca}$ reaction rate at stellar temperatures. The energies and proton branching ratios of several 36Ca levels that fall in the Gamow window for x-ray bursts were obtained. Using the empirical spectroscopic information and theoretical predictions of γ -decay widths, the reaction rate could be well constrained. The authors concluded that the ${}^{35}K(p, \gamma)$ ${}^{36}Ca$ reaction does not show a strong impact on the x-ray light curve. Similarly, the proton branching ratios of ²¹Na levels studied in the present work may provide useful information for the astrophysical $^{17}F(\alpha, p)$ ^{20}Ne rate determination. Informing such reaction rate calculations is beyond the scope of the present work.

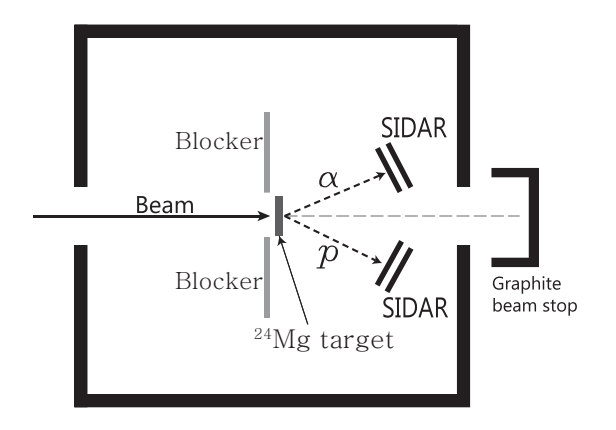


FIG. 1. A schematic diagram of the experimental setup for the 24 Mg $(p, \alpha)^{21}$ Na* $(p)^{20}$ Ne* measurement is shown.

II. EXPERIMENTAL SETUP

A schematic illustration of the 24 Mg(p, α) 21 Na*(p) 20 Ne* experimental setup is shown in Fig. 1. A 31-MeV proton beam was produced and accelerated from the 25-MV electrostatic tandem accelerator at the Holifield Radioactive Ion Beam Facility (HRIBF) of Oak Ridge National Laboratory (ORNL) [10] to bombard isotopically enriched (99.9%) 24 Mg solid targets. Recoiling α particles from the (p, α) reaction and decay protons from the 21 Na heavy recoil were detected at forward angles by the silicon detector array (SIDAR) [11]. The SIDAR was configured with four trapezoidal wedges of ΔE (100- μ m-thick) and E (1000- μ m-thick) telescopes. Each SIDAR detector is segmented into 16 annular strips. The angles covered by the SIDAR were from 17° to 44° in the laboratory frame. Light-charged particles from the reaction were identified using standard energy loss techniques.

A typical particle identification plot from the experiment obtained at $\theta_{lab} = 23.6^{\circ}$ is shown in Fig. 2. Events falling in

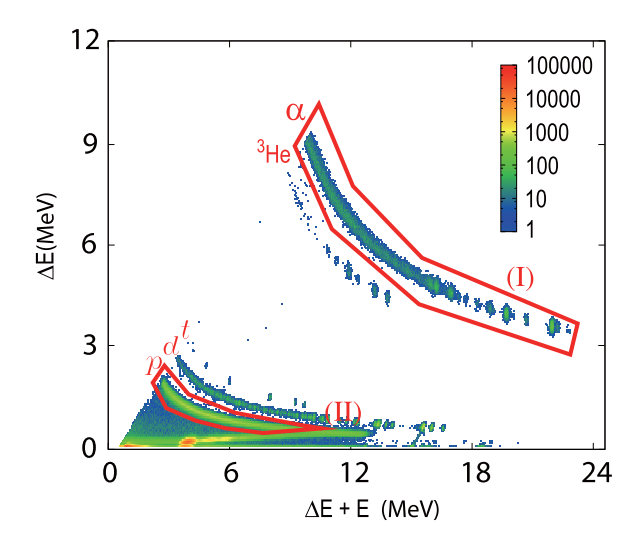


FIG. 2. Particle identification (energy loss vs total energy) plot obtained at $\theta_{\rm lab}=23.6^{\circ}$ from the $p+^{24}{\rm Mg}$ reaction. Events falling in the gates (I) and (II) are identified as the α particles and protons, respectively.

gates (I) and (II) are identified as the α particles and protons, respectively. As shown in the figure, the light-charged particles were clearly identified without significant evidence of contamination. Because the experimental setup parameters such as beam energy, target thickness, and detector thicknesses were optimized for the $^{24}{\rm Mg}(p,\alpha)^{21}{\rm Na}$ transfer reaction measurement, energetic protons with energies of approximately 7.2 MeV and greater punched through the E layer and caused the "back-bending" locus as shown in the figure. Therefore, only low-energy protons falling in gate (II) and the ones stopped in the ΔE detectors were considered in the present analysis. The validity of the choice of gate (II) is confirmed by Monte Carlo simulations using the computer code VIKAR (virtual instrumentation for kinematics and reactions) [12].

III. COINCIDENCE BETWEEN REACTION α PARTICLES AND DECAY PROTONS

To correctly estimate the energies of detected charged particles, the energy response of each silicon strip and associated electronic channel was calibrated using an α -emitting source composed of 239 Pu (5.157 MeV), 241 Am (5.486 MeV), and 244 Cm (5.805 MeV). Energy resolutions were measured to be approximately 1%. The calibrations were performed before and after the in-beam measurements to correct for any gain changes that might have occurred.

Because the energies of the reaction α particles observed in the (p, α) transfer reaction ranged from approximately 9.8 to 23.3 MeV, which is well above the energy calibration range of about 5 MeV, the α -energy spectrum obtained at each detector strip was internally calibrated using five strongly populated energy levels of ²¹Na: the ground state and excited states at $E_x = 0.332$, 2.798, 4.419, and 6.879 MeV. As described in Ref. [8], the internal energy calibration resulted in good agreement between the empirical excitation energies and literature values. Such additional energy calibrations could not be performed for the proton energies because the proton energy spectra obtained from the measurements were rather featureless. However, because the energies of the protons considered in the present analysis ranged from about 0.5 to 7.2 MeV, the α source calibrations worked well for the protons (see Sec. IV for details).

To identify events from the proton decay of radionuclide ²¹Na, we simultaneously detected the α particles from the $^{24}{\rm Mg}(p,\alpha)^{21}{\rm Na}$ transfer reaction and protons from the decay of ²¹Na. Events were considered to be coincident when two particles fell within a timing gate of about 4 μ s. Figure 3 shows the decay proton energy versus the coincident α -particle energy plot for all identified events. Several diagonal groups of events are evident in the figure. Events falling in the red, blue, and green gates are associated with decays to the ground state ($J^{\pi} = 0^{+}$), the first excited state ($E_x = 1.634$ MeV, $J^{\pi} = 2^{+}$), and the second excited state ($E_x = 4.247$ MeV, $J^{\pi} = 4^{+}$) of ²⁰Ne, respectively. Each group is labeled as p0, p1, or p2 in the figure. Several groups of events that originate from different ²¹Na states are clearly identified in the p1 = 0 and p1 gate. For example, the lower rightmost group in the p0 gate corresponds to the events from the decay of

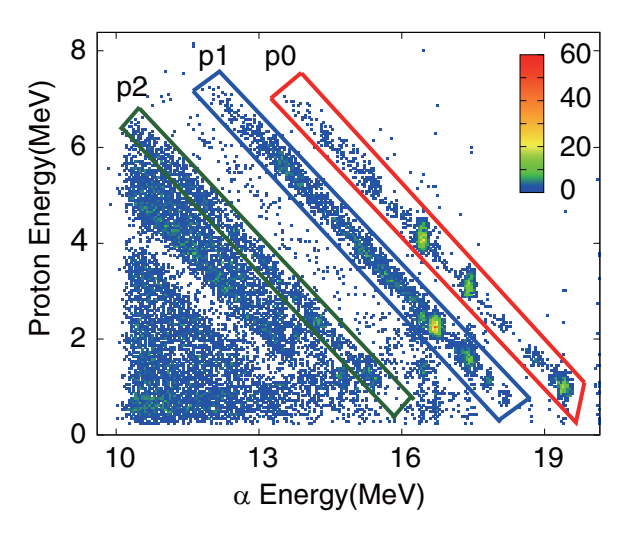


FIG. 3. The decay proton energy versus coincident α -particle energy plot is shown for all identified events. Events falling in the red, blue, and green gates are associated with the ground state (p0), the first excited state (p1), and the second excited state (p2) of 20 Ne, respectively.

the $E_x = 3.675$ MeV level in ²¹Na. Similarly, another intense group in the same gate that appears near the proton energy of 4 MeV represents the events from the $E_x = 6.879$ MeV level.

IV. BRANCHING RATIOS OF ²¹Na

Figure 4(a) shows the 21 Na excitation energy spectrum obtained from the 24 Mg (p,α) 21 Na reaction measurement [8].

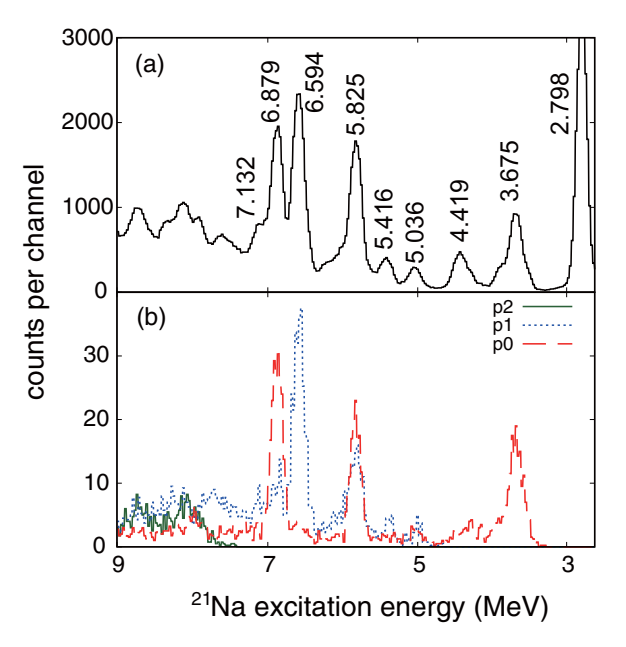


FIG. 4. (a) 21 Na excitation energy spectrum obtained from the 24 Mg(p, α) 21 Na reaction measurement [8]. Identified levels are labeled with their excitation energies. All energies are in MeV. (b) Spectra gated on decay proton coincidences. The spectra gated on the p0, p1, and p2 groups of Fig. 3 are shown as red dashed, blue dotted, and green solid lines, respectively.

Excitation energies are shown in MeV for the identified 21 Na levels. The α -energy spectra were first extracted from 16 angles. The α energies were internally calibrated at each angle and then converted to the 21 Na excitation energy using the known detector geometry and reaction kinematics. The figure is the resultant energy spectrum summed over all angles.

Figure 4(b) was obtained by requiring decay protons in coincidence with α particles populating states in 21 Na. The spectra gated on the p0, p1, and p2 groups of Fig. 3 (populating the ground, first excited, and second excited states in 20 Ne, respectively) are shown. Energy levels located below $E_x \approx 3$ MeV could not be observed in the present work owing to the proton threshold energy of 21 Na (2.432 MeV) and the discriminator threshold. As shown in Fig. 4, three 21 Na energy levels located at $E_x = 3.675$, 5.825, and 6.879 MeV were clearly identified in the p0-gated spectrum. Similarly, two peaks associated with $E_x = 5.825$ and 6.594 MeV levels in 21 Na were evident in the p1-gated spectrum. No obvious structure was observed for the p2 group.

The proton branching ratios associated with the p0 (B_{p_0}) and p1 (B_{p_1}) channels for observed ²¹Na energy levels were determined from the ratio of the number of proton-gated decay events [Fig. 4(b)] to the number of times each level was populated, the (p, α) singles events [Fig. 4(a)], after adjusting each for their relative detection efficiencies. The results are summarized in Table I. Although the p2 channel is clearly shown in Fig. 3, the branching ratios B_{p_2} could not be extracted due to poor statistics. The geometric detection efficiency was considered in branching ratio calculations because not all protons from the decay were detected by the silicon detector array. The solid angle subtended by the SIDAR was 0.61 sr, which corresponds to about 5% coverage of 4π . Our determination of a proton branching ratio value for the 3.675-MeV level of 0.93, for example, shows that this level will overwhelmingly undergo proton decay, with only a 7% probability for γ decay; the excitation energy of this level is too low for other decay channels such as α or neutron to be open.

To obtain the precise number of counts for each level identified in the spectrum gated on decay proton coincidences, several background mechanisms were considered. Some background coincidences attributed to the rather long timing gate of about 4 μ s was evident as shown in Fig. 3. By implementing a two-dimensional gate with size and shape similar to those of the p0 gate at a slightly higher α -energy region, where particle decay is energetically forbidden, the level of background events was estimated. The result shows that the probability of background coincidence is only about 5%.

As previously done in Refs. [8,14], possible contaminations in the 24 Mg solid targets, such as 12 C, 14 N, and 16 O, were thoroughly investigated as well. Kinematics calculations show that the 14 N(p, α) 11 C*(p) 10 B and 16 O(p, α) 13 N*(p) 12 C* channels associated with the ground state of 10 B and the first excited state of 12 C, respectively, can produce decay protons at the energies relevant for the p1 group and the region between p1 and p2 groups of the present work. Although no obvious events from the contaminations were evident in the α -energy spectrum, the rather high level of background was observed

TABLE I. Extracted proton branching ratios of the observed ²¹Na energy levels are summarized for the p0 (B_{p_0}) and p1 channel (B_{p_1}). The threshold for the p0 (p1) channel is located at $E_x = 2.432$ (4.066) MeV. Excitation energies and spin values are taken from Ref. [8] unless otherwise noted.

E_x (MeV)	J^{π}	B_{p_0}	B_{p_1}
3.675 ^a	3/2 ^{-b}	0.93 ± 0.30	_
4.419	$(3/2, 5/2)^+$	0.12 ± 0.04	
5.036	$(3/2, 5/2)^+$	0.29 ± 0.09	0.31 ± 0.10
5.416	1/2+	0.03 ± 0.01	0.23 ± 0.07
5.825	7/2 ^{-b}	0.67 ± 0.20	0.51 ± 0.15
6.594	$(3/2, 5/2)^+$ or $[(1/2, 3/2)^- + (7/2, 9/2)^+]$	0.01 ± 0.002	0.92 ± 0.28
6.879	$3/2^{-b}$	1.12 ± 0.34	0.11 ± 0.03
7.132	$1/2^+$ or $(1/2, 3/2)^-$	0.05 ± 0.01	0.43 ± 0.13

^aThe energy of the level is reported to be 3678.9(4) keV in Ref. [13].

between the p1 and p2 gates in Fig. 3. Therefore, another two-dimensional gate was implemented in this area for better estimations of background events, which affects the proton branching ratios associated with the p1 channel.

Isotropic decay in the center of mass (c.m.) frame was assumed for the branching ratio calculations. A simple test was used to evaluate the assumption of isotropy. As shown in Fig. 4(b), for instance, decay protons from the 5.825-MeV state were clearly identified in both the p0 and p1 channels. For each identified decay event, the relative angle between the recoiling α particle and the decay proton was deduced using the strip number and the detector wedge number (i.e., the polar angle and the azimuthal angle). The normalized intensities of proton decays from the 5.825-MeV level plotted as a function of the relative angle for the p0 and p1 channels are shown in Fig. 5(a). Although the spin values of the ²⁰Ne levels associated with each channel are different— $J^{\pi} = 0^{+}$ and 2^{+} for the p0 and p1 channels, respectively—the curves show very similar patterns over the relative angle range, which means the decay can be reasonably approximated as isotropic. Additional support for the isotropy can be found in Figs. 5(b) and 5(c), which show the normalized intensity plots for the 6.594and 6.879-MeV levels, respectively. Because the distribution for the 6.594-MeV (6.879-MeV) level extracted from the p0 (p1) channel was rather featureless because of low statistics, a comparison between the normalized intensities obtained from both channels could not be made. Therefore, another test was implemented for the isotropy evaluation. By considering all possible combinations of the detector strip hits, a relative angle histogram for isotropic decay was obtained as shown in Figs. 5(b) and 5(c). A relative angle histogram for anisotropic decay assuming a cosine variation among many different possible variations is also shown in Figs. 5(b) and 5(c). No significant difference was observed between the data and the expectations for isotropic decay. It is therefore a reasonable approximation to treat the decay as largely isotropic. As previously reported [4–6], a conservative systematic uncertainty of 30% was introduced to account for any discrepancies between isotropic and anisotropic decays, which was the dominant uncertainty in extracted proton branching ratios.

In recent work by Lund *et al.* [15], β -delayed proton emissions from ²¹Mg were measured to study the decay scheme. A total of 27 branches were observed at the energy range of $E_{\text{c.m.}} = 0.4$ –7.2 MeV. Relative intensities of identified decay channels were reported. Similarly, Wang *et al.* [16] also reported results from a β -delayed particle emission experiment. Together with a silicon detector array for charged-particle detection, high-purity germanium detectors were used to detect the γ rays emitted from the decay. Characteristic 1.633-MeV γ rays originating from the deexcitation of the first excited state in ²⁰Ne were clearly observed, which results

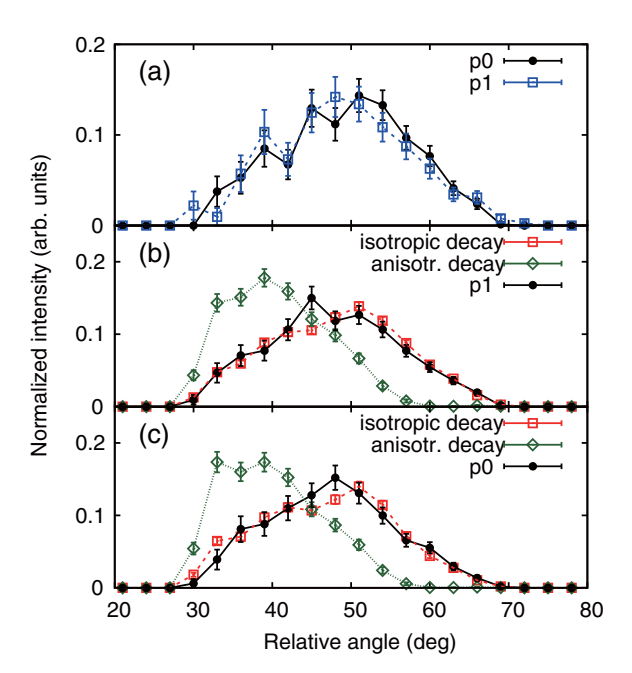


FIG. 5. Normalized intensity of proton decays from the 5.825-MeV level as a function of relative angle for the p0 (black solid line) and p1 (blue dotted line) channels in panel (a). Similarly, the empirical intensities for the 6.594- and 6.879-MeV levels are shown as a black solid line in panels (b) and (c), respectively. The calculated distributions assuming isotropic and anisotropic decay are shown as red dashed and green dotted lines, respectively.

^bTaken from Ref. [13].

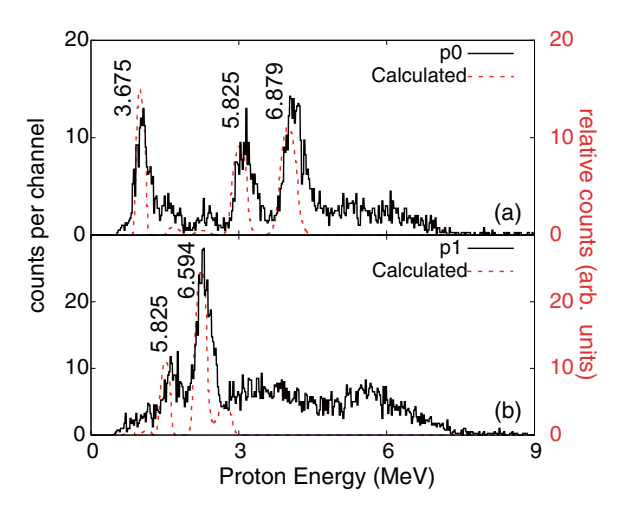


FIG. 6. Proton energy spectra are shown as black solid lines for the coincident events falling in the p0 (a) and p1 (b) gates. Several apparent peaks associated with 21 Na levels are labeled with their excitation energies in MeV. Expected proton energy spectra are also shown in the figure as red dotted lines.

in an improved proton spectrum coincident with γ rays. By considering the excitation energies and spins of reported levels, it can be concluded that the 5.036-MeV level of the present work likely corresponds to levels previously identified in the β -delayed proton emission measurements: $E_x =$ 5.020(9) MeV in Ref. [15] and 5.013(20) MeV in Ref. [16]. However, the interpretations of the level are different to some extent. Lund et al. [15] concluded that the decay protons with energies of about $E_p = 2.587$ MeV are associated with the level. The protons then should be the result of the p0 channel. No protons related to the p1 channel were identified. On the other hand, Wang et al. [16] concluded that the protons at the energies of about 0.987 MeV produced through the p1 channel are the evidence of the level. No events from the p0channel could be identified. The proton branching ratios of the p0 and p1 channels obtained from the present work, 0.29(9) and 0.31(10), respectively, however, are still different from previous results. Further high-resolution decay spectroscopy is encouraged to resolve this discrepancy.

Because internal energy calibrations could not be performed for proton energies as mentioned above, the validity of using the energy calibration obtained from an α -emitting source was investigated using proton energy spectra. The proton energy spectra of coincident events for the p0 and p1 gates are shown in Fig. 6. The corresponding spectrum for the p2 channel could not be obtained due to poor statistics. Several peaks associated with ²¹Na levels are labeled with their excitation energies in MeV. The expected proton energy spectra obtained by assuming the production of ²¹Na levels through the 24 Mg(p, α) 21 Na reaction and isotropic decay are also shown in the figure as red dotted lines. The detector geometry and reaction kinematics of the experiment, typical silicon detector energy resolution of about 5%, proton branching ratios obtained from the present work, and relative cross sections of various ²¹Na energy levels reported in Ref. [8] were considered in the calculations. As shown in Fig. 6, the

TABLE II. Proton decay of excited states in 21 Na to the ground and first excited ($E_x = 1.634$ MeV) states in 20 Ne. Observed and calculated proton energies and their uncertainties are summarized for five identified transitions. All energies are in MeV.

Transition	E_p observed	E_p calculated
$3.675 \rightarrow 0.000$	1.06 ± 0.34	1.01 ± 0.17
$5.825 \rightarrow 0.000$	3.14 ± 0.43	2.99 ± 0.28
$6.879 \rightarrow 0.000$	4.16 ± 0.55	3.99 ± 0.29
$5.825 \rightarrow 1.634$	1.65 ± 0.41	1.50 ± 0.17
$6.594 \rightarrow 1.634$	2.33 ± 0.41	2.23 ± 0.22

empirical proton energy spectra can be well reproduced by calculations, demonstrating that the energy calibrations obtained from the α -source calibration are appropriate. Larger widths for the empirical proton spectra are caused by the lack of internal energy calibrations mentioned above. Observed and calculated proton energies and their uncertainties are summarized in Table II for five identified transitions.

V. DISCUSSION

The proton branching ratios obtained from the present work may also be useful to constrain spins and parities of the populated levels. For instance, the spin of the 4.419-MeV level was constrained to be $(3/2^+, 5/2^+)$ in Ref. [8] by comparing the empirical angular distribution of deuterons from the $^{24}\text{Mg}(p,\alpha)^{21}\text{Na}$ reaction and the results of theoretical DWBA calculations. In the latest compilation, however, $J^\pi=11/2^+$ is assigned for the level [13]. Because the proton decay through the p0 channel (i.e., the decay channel to the $J^\pi=0^+$ ground state of ^{20}Ne) was clearly observed in the present work with $B_{p0}=0.12\pm0.04$, high spin values for the level would be less probable. Therefore, the spin value of $3/2^+$ or $5/2^+$ for the 4.419-MeV level is proposed in the present work.

Another example can be found in the cases of the energy levels with the same spin values. The spins of the energy levels at $E_x = 3.675$ and 6.879 MeV are known to be $3/2^-$. The branching ratios of the levels show that the decay favors the p0channel as summarized in Table I. Although the proton decays from only eight ²¹Na energy levels are studied in the present work, this may prove that the proton decays are quite selective. Two ²¹Na levels at $E_x = 6.594$ and 7.132 MeV were observed for the first time in Ref. [8]. The spin of the 7.132-MeV level was constrained to be $1/2^+$ or $(1/2, 3/2)^-$. If the proton branching ratios are indeed sensitive to the spin values, the possibility of $J^{\pi} = 3/2^{-}$ could be ruled out because the B_{p_0} value of the level is measured to be 0.05 ± 0.01 . Moreover, because the ratio of B_{p_0} to B_{p_1} for the level is similar to that of the well-known 5.416-MeV ($J^{\pi} = 1/2^{+}$) level, the spin of the level is possibly $1/2^+$. In the case of the other new level at 6.594 MeV, the proton decay through the p1 channel is very strong ($B_{p_1} = 0.92 \pm 0.28$). Because no other observed level shows the B_{p_1} value close to 1, we cannot further constrain the spin of the 6.594-MeV level through the present work.

VI. CONCLUSION

Decay protons from the 24 Mg(p, α) 21 Na*(p) 20 Ne* channel were investigated to obtain proton branching ratios of excited states populated in 21 Na. Proton beams of 31 MeV from the HRIBF of ORNL bombarded isotopically enriched 24 Mg solid targets. This is a follow-up analysis of previously reported [8] measurements of this reaction. By requiring coincidences between reaction α particles and decay protons, three groups of events associated with the ground state (p0), the first excited state (p1, E_x = 1.664 MeV), and the second excited state (p2, E_x = 4.247 MeV) in 20 Ne were identified.

Proton decay branching ratios for excitations in 21 Na were extracted from coincidences between protons and reaction α particles from the $p+^{24}$ Mg measurement. Isotropic decay in the center of mass frame was assumed for the branching ratio calculations. A total of 14 branching ratios were extracted: 8 branching ratios from the p0 channel and 6 branching ratios from the p1 channel. Evidence of proton decay of 21 Na excitations to higher-lying states in 20 Ne was observed. However, branching ratios associated with the channels to the second excited 20 Ne state (p2) and higher 20 Ne states could not be extracted due to poor statistics. In a future work, we will use

our results, along with other considerations, to determine a new 17 F(α , p) 20 Ne reaction rate.

ACKNOWLEDGMENTS

This work was supported by National Research Foundation of Korea (NRF) grants funded by the Korea government (MSIT) (Grants No. 2013M7A1A1075764, No. 2016R1A5A1013277, No. 2020R1A2C1005981, and No. 2020R1I1A1A01065120). This research was supported in part by the National Nuclear Security Administration under the Stewardship Science Academic Alliances program through U.S. DOE Cooperative Agreement No. DE-FG52-08NA28552 with Rutgers University and Oak Ridge Associated Universities. This work was also supported in part by the Office of Nuclear Physics, Office of Science of the U.S. DOE, under Contract No. DE-FG02-96ER40955 with Tennessee Technological University, Contract No. DE-FG02-96ER40983 with the University of Tennessee, and Contract No. DE-AC-05-00OR22725 with Oak Ridge National Laboratory; by the National Science Foundation under Contract No. PHY-1713857 with University of Notre Dame and Contract No. PHY-1812316 with Rutgers University; and by the Institute for Basic Science (Grant No. IBS-R031-D1).

^[1] D. W. Bardayan, J. Phys. G: Nucl. Phys. 43, 043001 (2016).

^[2] W. P. Tan, J. L. Fisker, J. Gorres, M. Couder, and M. Wiescher, Phys. Rev. Lett. 98, 242503 (2007).

^[3] C. M. Deibel, J. A. Clark, R. Lewis, A. Parikh, P. D. Parker, and C. Wrede, Phys. Rev. C 80, 035806 (2009).

^[4] K. A. Chipps et al., Phys. Rev. C 82, 045803 (2010).

^[5] K. A. Chipps et al., Phys. Rev. C 86, 014329 (2012).

^[6] K. A. Chipps et al., Phys. Rev. C 95, 044319 (2017).

^[7] D. W. Bardayan et al., J. Phys.: Conf. Ser. 1308, 012004 (2019).

^[8] S. M. Cha et al., Phys. Rev. C 96, 025810 (2017).

^[9] L. Lalanne et al., Phys. Rev. C 103, 055809 (2021).

^[10] J. R. Beene et al., J. Phys. G: Nucl. Part. Phys. 38, 024002 (2011).

^[11] D. W. Bardayan *et al.*, Phys. Rev. C **63**, 065802 (2001).

^[12] https://sites.google.com/a/nuclearemail.org/vikar/.

^[13] R. B. Firestone, Nucl. Data Sheets 127, 1 (2015).

^[14] M. S. Kwag et al., Eur. Phys. J. A 56, 108 (2020).

^[15] M. V. Lund et al., Eur. Phys. J. A 51, 113 (2015).

^[16] Y. Wang et al., Eur. Phys. J. A 54, 107 (2018).